Hyperspectral Imaging via Three-dimensional Compressed Sampling*

Li Wang, Yan Feng

Department of Electronics and Information Northwestern Polytechnical University, ShaanXi, China
wangli871016@163.com, sycfy@nwpu.edu.cn

Abstract - Hyperspectral images (HSI) are a collection of hundreds of images which have been acquired simultaneously in narrow and adjacent spectral bands. Aimed at meeting the needs of real-time process of hyperspectral data, the development of compressive techniques before the transmission and storage becomes critical. Recently, Compressed Sampling (CS), which exploits the sparsity of signals, has been allowed to reconstruct signals with fewer measurements than the traditional Nyquist sampling approach. In order to make use of the spectral correlation and spatial correlation simultaneously in the compressed sampling process, in this paper we developed a new three-dimensional compressed sampling (3DCS) method to reduce the sampling rate. In 3DCS, the three-dimensional circulant sampling model is presented, which samples the hyperspectral images with a random convolution process and a band-varying subsampling. In addition, an efficient reconstruct algorithm called three-dimensional total variation (3DTV) by exploiting its spatial and spectral correlation is used for this 3DCS with guaranteed convergence. The experiment results demonstrate that the superiority of our proposed 3DCS over 2DCS which only makes uses the spatial correlation is in terms of high recovery accuracy with respect to the sampling rate. And the reconstruct image using our proposed 3DCS is much better than the traditional 2DCS.

Index Terms - Hyperspectral imaging, Compressed sampling, 3DCS, 3DTV

I. Introduction

Hyperspectral images (HSI) are a collection of hundreds of images that have been acquired simultaneously in narrow and adjacent spectral bands, typically by airborne sensors. HSI are produced by expensive spectrometers that sample the light reflected from a two-dimensional area with increasing spatial resolution and spectral resolution. A HSI data set is thus a "cube" with two spatial dimensions and one spectral dimension. Hyperspectral imaging has many applications including environmental monitoring, agriculture planning or mineral exploration. Regrettably, the sheer volume of data makes acquisition, transmission, storage and analysis of HSI computationally very challenging. So how to manipulate HSI via a suitable compressive technique becomes critical. Therefore, the problem addressed in this paper is how to reduce the sampling rate to meet the needs of real-time process and the data storage, transmission.

The traditional sampling theoretical foundation is the Nyquist sampling theorem, which states that the signal information is preserved if the underlying analog signal is uniformly sampled above the Nyquist rate, which is twice its highest analog frequency. Unfortunately, Nyquist sampling has two major shortcomings when applied in hyperspectral imaging. First, acquisition of HSI needs a large sensor. This may be infeasible or extremely expensive. Second, the raw data acquired by Nyquist sampling is too large to acquire and transmit in short time.

However, recent developments in the field of compressed sampling (CS) [1] [2] offer an attractive potential solution to this problem. The core idea of compressed sampling is that if a signal or image of interest is sparse or compressible in some domain, then it can be reconstructed accurately from very few (relative to the dimension of the signal or image) non-adaptive measurements [3]. It is advantageous over Nyquist sampling, because it can relax the computational burden during sensing, and acquire high resolution data using small sensors. CS offers many advantages such as the possibility of hardware simplification, reduction of data acquisition times, achieving high resolution, and signal compression.

Assume a vectorized image or signal x of size L is sparsely represented as $x = \Psi z$, where z has K non-zero entries (called K -sparse) and Ψ is the wavelet transform. Compressed Sampling acquires a small number of incoherent linear projections $b = \Phi x$ and decodes the sparse solution $z = \Psi^T x$ as follows:

$$\min_z \|z\|_1 \qquad s.t. \quad Az = \Phi\Psi z = \Phi x = b. \qquad (1)$$

Where, Φ is a random sampling (RS) [4] ensemble. Recently, circulant sampling (CirS) [5] was introduced to replace RS with the advantages of easy hardware implementation, memory efficiency and fast decoding. It has been shown that CirS is competitive with RS in terms of recovery accuracy [5].

CS often reduces the required sampling rate by seeking the sparsest representation or by exploring some prior knowledge of the signal. Image CS (called 2DCS) samples each image independently and reconstructs each image by minimizing its total variation [6]. J. E. Fowler has proposed a method using JPEG2000 and principal component analysis in hyperspectral image compression [7] and use CPPCA to reconstruct hyperspectral image in the receiver-side [8]. Distributed CS of Hyperspectral image via blind source separation is proposed in [9] to achieve a higher peak signal-to-noise ratio (PSNR) than other CS methods. A new reconstruction algorithm based on interband prediction and joint optimization is proposed by Haiying Liu, in which linear

*This work is supported by the National Natural Science Foundation of China under grant 61071171.

prediction is first applied to remove the correlations among successive hyperspectral measurement vectors [10].

However, the existing methods often consider the highly spectral correlation between adjacent bands in the reconstruct process and the sampling rate in the sample process is still quite high. These methods could not fully utilize the spectral correlation. So in this paper, we take advantage of a circulant convolution matrix as well as a band-varying subsampling matrix in the sampling process utilizing the spectral correlation to reduce the sampling rate, and introduce 3DTV as the regularization term to reconstruct the hyperspectral image from the incomplete sampled data.

This paper is organized as follows. Section 2 presents the proposed 3DCS, consists of 3D CirS and three-dimensional total variation (3DTV). In this section, the recovery algorithm for the 3DCS and the exact solution steps are also developed. Experimental results are given in Section 3 to show the superiority of our 3DCS in terms of high PSNR followed by concluding remarks in Section 4.

II . Proposed method

A. *Overview of our 3D Compressive Sampling (3DCS)*

In this section, the overview of our 3D compressed sampling (3DCS) consisting of 3D Circulant Sampling and its efficient reconstruct algorithm is given for a Hyperspectral data cube as shown in Fig. 1. The hyperspectral data is represented as a matrix $I=[I_1,...,I_k,...,I_T]$, where column I_k denotes the k-th band (the pixels in band k reorders in column-wise). Using 3D CirS, the hyperspectral image has been sampled to incomplete data and in the reconstruct process, each image is recovered by jointly reconstruction algorithm by minimizing its three-dimensional total variation (3DTV).

This 3DCS is motivated by two characteristics of hyperspectral images. First, hyperspectral images are often piecewise smooth in 2D spatial domain and spectral domain. Second, the adjacent bands in a hyperspectral data are highly correlated in the spectral dimension, which can be modeled as a low-rank matrix with sparse innovations.

B. *3D Circulant Sampling*

Hyperspectral data are highly compressible with two-fold compressibility: (1) each spatial image is compressible, and (2) the entire cube, when treated as a matrix, is of low rank. To fully exploit such rich compressibility, in this paper we propose a new scheme that never requires to explicitly store or process a hyperspectral cube itself. The 3D circulant sampling (CirS) consists of two steps:

1) Random convolution. 3D CirS convolves a band image I_k by a random kernel H, denoted by CI_k, where C is a circulant matrix with H as its first column. C is diagonalized as $C=F^{-1}diag\left(\hat{H}\right)F$, where $\hat{H}$ is the Fourier transform of H, denoted by $\hat{H}=FH$.

2) Random subsampling. It consists of random permutation (P) and band-varying subsampling (S_k). S_k selects a block of M pixels from all N pixels on PCI_k and obtains the data $B_k=S_kPCI_k$. Note that the selected block drifts with band k (Fig. 1). To relax the burden of both sampling and reconstructing, it is desirable to implement a physical mapping from a random subset to a 2D sensor. Although it is challenging, a possible solution is to implement random permutation by a bundle of optical fibers, followed by a moving small sensor. The easy way—sensing the whole image CI_k by a big sensor and throwing away the unwanted $N-M$ pixels does not benefit sensing but yields a method of computation-free sampling.

As shown in Fig. 1, the 3D circulant matrix is denoted as $\overline{\Phi}=diag(\Phi_1,\Phi_2,...,\Phi_T)$, and $[B_1;B_2;...;B_T]$ is the sampled data.

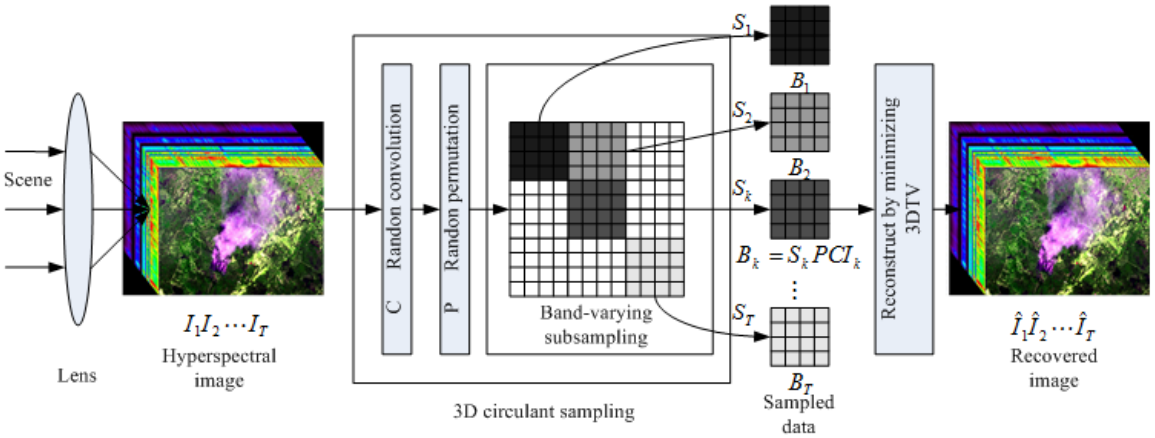

Fig. 1 The framework of Hyperspectral Imaging using the proposed 3DCS. A lens (for collected the hyperspectral image, vectorized as $I_k, 1\le k\le T$) is followed by 3D circulant sampling, which consists of random convolution (C), random permutation (P) and band-varying subsampling (S_k). From the sampled data $B_k=S_kPCI_k, 1\le k\le T$, the hyperspectral image $\hat{I}_k, 1\le k\le T$ is reconstructed by minimizing 3DTV.

C. Three-dimensional Total Variation (3DTV)

In this section, 3DTV is presented in detail. In the 2D image CS, in order to use the piecewise smoothness in the spatial domain, the total variation (TV) is often used to recover the image from incomplete measurements. The widely-used form of TV is $TV_{l_1 l_2}$ [11] [12], which is defined as all pixels of the discrete model and gradient vector:

$$TV_{l_1 l_2}(f) = \sum_{i,j} \sqrt{\left(D_{h,ij} f\right)^2 + \left(D_{v,ij} f\right)^2} . \tag{2}$$

$$D_{h,ij} f = \begin{cases} f_{i+1,j} - f_{i,j} & i < n \\ 0 & i = n \end{cases} . \tag{3}$$

$$D_{v,ij} f = \begin{cases} f_{i,j+1} - f_{i,j} & j < n \\ 0 & j = n \end{cases} . \tag{4}$$

Where, f is the 2D image and n is the size of the image.

In reference [13], the l_1 -norm based TV measure $TV_{l_1}(f) = \|D_h f\|_1 + \|D_v f\|_1$ is proven to be better than $TV_{l_1 l_2}$ in reducing the sampling rate, where D_h is the horizontal gradient operator and D_v is the vertical gradient operator. Here, the highly spectral correlation between adjacent bands is considered and the total variation in the spectral dimension can also be a constraint in the reconstruct optimization problem. Extending TV_{l_1} to the three-dimensional (spatial and spectral) domain, our 3DTV is formulated as:

$$3DTV(I) = \sum_{k=1}^{T} \left(\|D_h I'_k\|_1 + \|D_v I'_k\|_1 + \rho \|D_\lambda I'_k\|_1 \right) . \tag{5}$$

Where, D_h and D_v is the same as before, D_λ is the gradient operator in the spectral dimension and ρ is proportional to the spectral correlation, I'_k is the image of band k, which is denoted as I_k, has been reshaped into a 2D matrix.

D. 3DCS Recovery Algorithm

In this section, an efficient reconstruct algorithm is presented to reconstruct the hyperspectral image from the sampled data. There are many reconstruct algorithms that often use l_1 -norm as the regularization term. Here, we use the three-dimensional total variation (3DTV) as the regularization term in the recovery algorithm. Therefore, our recovery algorithm is to solve the following optimization:

$$\min_I \quad 3DTV(I) \quad s.t. \quad \bar{\Phi} I = B . \tag{6}$$

By introducing weight parameters $\alpha_h = \alpha_v = 1$, $\alpha_\lambda = \rho$ and auxiliary parameters $\chi = (G_h, G_v, G_\lambda, R)$, our 3DCS using (5) can be rewritten as:

$$\begin{aligned} \min_{I, G_h, G_v, G_\lambda} \quad & \alpha_h \|G_h\|_1 + \alpha_v \|G_v\|_1 + \alpha_\lambda \|G_\lambda\|_1 \\ s.t. \quad & G_h = D_h I, G_v = D_v I, G_\lambda = D_\lambda I \\ & R_k = C I_k, S_k P R_k = B_k \end{aligned} . \tag{7}$$

This linearly constrained problem can be solved by augmented Lagrangian multipliers (ALM) [11]. Given an l_1 -norm problem:

$$\min \|a\|_1 \ s.t. \ a = b . \tag{8}$$

Its augmented Lagrangian function (ALF) is defined as:

$$L_\beta(a, b, y) = \|a\|_1 - y\beta(a - b) + \frac{\beta}{2} \|a - b\|_2^2 . \tag{9}$$

Then, the ALF of (7) is written as:

$$\begin{aligned} L(I, G, R, b, g) = & \alpha_h \left(\|G_h\|_1 + \beta_h \|G_h - D_h I - b_h\|_2^2 \right) \\ & + \alpha_v \left(\|G_v\|_1 + \beta_v \|G_v - D_v I - b_v\|_2^2 \right) \\ & + \alpha_\lambda \left(\|G_\lambda\|_1 + \beta_\lambda \|G_\lambda - D_\lambda I - b_\lambda\|_2^2 \right) \\ & + \beta_4 \left\| R - \bar{C} I - g \right\|_2^2 \\ & s.t. \quad S_k P R_k = B_k, 1 \le k \le T \end{aligned} \tag{10}$$

Where, $G = \{G_h, G_v, G_\lambda\}$, $b = \{b_h, b_v, b_\lambda\}$, $\beta_h, \beta_v, \beta_\lambda, \beta_4$ are over-regularization parameters, $\gamma = (b_h, b_v, b_\lambda, g)$ is Lagrangian multipliers and $\bar{C} = diag(C, ..., C)$.

The objective function (10) is actually a two optimization sub-problems, namely, the minimization problem about χ and I . The operator splitting method [14] can convert a complex problem into multiple simple iterative solutions of sub-problems, so that each sub-problem contains only one variable. Using operator splitting method to solve (10), the specific iteration steps are as follows:

1) Separate Rectification: Solve χ^{i+1},

$$\chi^{i+1} = \arg\min_\chi L\left(I^i, \chi, \gamma^i\right) . \tag{11}$$

2) Joint reconstruction: Solve I^{i+1},

$$I^{i+1} = \arg\min_I L\left(I, \chi^{i+1}, \gamma^i\right) . \tag{12}$$

3) Update γ :

$$\begin{aligned} b_h^{i+1} &= b_h^i - \tau\left(G_h^{i+1} - D_h I^{i+1}\right) \\ b_v^{i+1} &= b_v^i - \tau\left(G_v^{i+1} - D_v I^{i+1}\right) \\ b_\lambda^{i+1} &= b_\lambda^i - \tau\left(G_\lambda^{i+1} - D_\lambda I^{i+1}\right) \\ g^{i+1} &= g^i - \tau\left(R^i - \bar{C} I^{i+1}\right) \end{aligned} . \tag{13}$$

Where, τ is the step length, i is the iteration number.

The convergence of the ALM requires an exact solution to $\arg\min_\chi L\left(I^i, \chi, \gamma^i\right)$ at each iteration, which can be obtained separately with respect to G and R .

Define a soft shrinkage function:

$$S\left(X, \frac{1}{\beta}\right) = \max\left\{ abs(X) - \frac{1}{\beta}, 0 \right\} \cdot \operatorname{sgn}(X) . \tag{14}$$

Where "•" denotes elementwise multiplication, and then G is straightforwardly updated by:

$$\begin{aligned} G_h^{i+1} &\leftarrow S\left(D_h I^i + b_h^i, 1/\beta_h\right) \\ G_v^{i+1} &\leftarrow S\left(D_v I^i + b_v^i, 1/\beta_v\right) \\ G_\lambda^{i+1} &\leftarrow S\left(D_\lambda I^i + b_\lambda^i, 1/\beta_\lambda\right) \end{aligned} \quad . \tag{15}$$

The complete circulant samples $R = [R_1; ...; R_T]$ are rectified by 3D data I^i and partial circulant samples B_k.

$$\begin{aligned} R_k^{i+1} &\leftarrow CI_k^i \\ R_k^{i+1}(Picks_k, :) &\leftarrow B_k \end{aligned} \quad . \tag{16}$$

Where, $Picks_k$ are the indices of rows selected by S_k.

III. Experimental Results

Our proposed 3DCS approach is evaluated on two hyperspectral images cube. The first cube is the scene of city Changzhou supported by Shanghai Institute of Technical Physics, Chinese Academy of Sciences and the office 308 of National 863 program which has 64 bands. The second is the cuprite scene from AVIRIS (http://www.airs.jpl.nasa.gov) and we intercept 64 bands to test. In this paper, sub-region is selected to simulate, and the size is 256*256 for each image. In the following paper, the first data set is denoted as scene1, while the second is scene2.

The first feature of our 3D CirS is the choice of the random kernel which is illustrated in Fig.1. In order to choose an appropriate random kernel to improve the recovery accuracy, six different convolution kernels are tested in the paper, such as the random Gauss matrix, the Bernoulli matrix, the orthonormal matrix, the hadamard matrix, the toeplitz matrix and the sparsity random matrix. The average PSNR of all bands using these six kernels at different sampling rate has been computed and the curve is given in Fig. 2. The figure depicts that the gauss kernel has the highest accuracy over other kernels regardless of sampling rate. So in the following experiments, we all choose the gauss kernel as the random kernel in the 3D CirS process.

There are two methods used in the experiments, (1) our proposed 3DCS, utilizing the spectral correlation and spatial correlation simultaneously; (2) traditional 2DCS, only using the spatial correlation in the sampling process. The methods are evaluated on scene1 and scene2 and we only show the PSNR of all the bands of scene2 in Fig. 3. The sampling rate of the two methods is $M/L = 20\%$.The figure reveals that our proposed 3DCS achieves higher average recovery accuracy than the 2DCS method. The average PSNR of our proposed method 3DCS is 38.4973 dB while the PSNR of 2DCS is 30.1374 dB. This demonstrates that when spectral correlation is considered in the sampling process, the reconstruct image can have a higher quality.

In order to compare the quality of the reconstruct images directly, the reconstructed images of the 30th band of scene1 at sampling rate 30% is given in Fig. 4. The original image of scene1 is displayed in the first row, while the reconstructed image using 2DCS is displayed on the left of the second row, and 3DCS on the right. We also give the PSNR of the reconstructed image of the specific band. It reveals that method 3DCS has a great advantage at improving PSNR and the details of the image are reconstructed better than 2DCS.

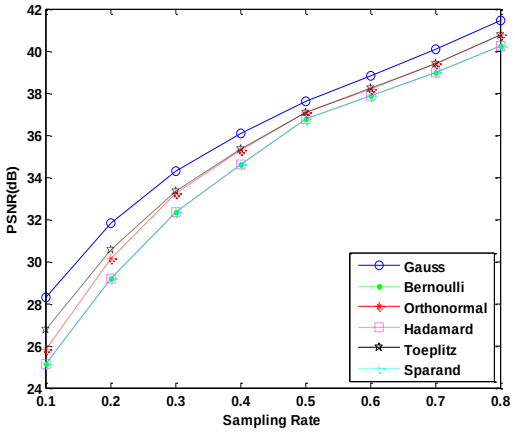

Fig. 2 Average PSNR of six convolution kernels using 3DCS. (Six kernels: Gauss matrix, Bernoulli matrix, Orthonormal matrix, Hadamard matrix, Toeplitz matrix and Sparsity random matrix)

By varying the sampling rate, our 3DCS algorithm and 2DCS is tested on the hyperspectral images. As shown in Fig. 5, the PSNR is the average of all the bands at each sampling rate. We only give the result of scene2 for the lack of space. Note that, in these two methods, the sampling rate varies from 0.1 to 0.5. The quality of the reconstruct image should be better than 2DCS because our method has sampled the spectral information between adjacent bands. As expectedly, our proposed method 3DCS has higher PSNR of the reconstruction image regardless of the sampling rate. Especially at the lower sampling rate, such as 10%, the superiority of 3DCS over 2DCS can be up to 6.5577dB.

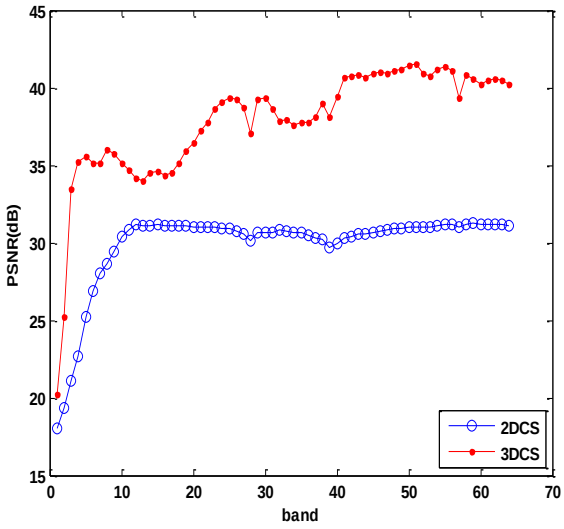

Fig. 3 The PSNR of the reconstructed image using two methods for scene2 at sampling rate 20%. (Average PSNR: 2DCS: 30.1374 dB, 3DCS: 38.4973 dB)

Fig. 4 The reconstructed image of scene1 using two methods at sampling rate 30%. (First row: Original image; Second row: Reconstruct images.) Reconstruct image PSNR: 2DCS (left): 24.7726 dB, 3DCS (right): 34.0355 dB)

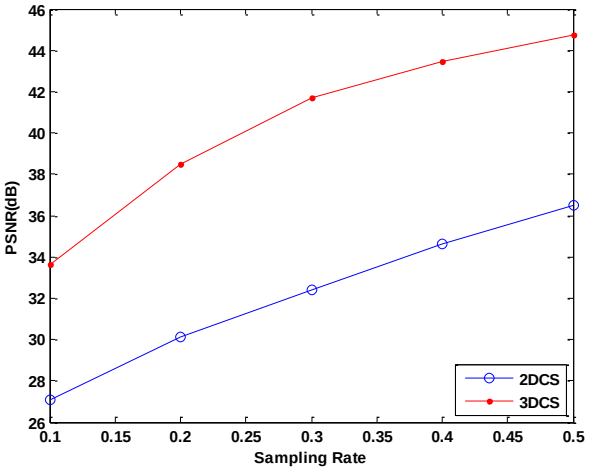

Fig. 5 Average recovery PSNR of all bands at different sampling rate for scene2.

IV. Conclusion

In this paper, a three-dimensional compressed sampling (3DCS) method has been proposed to compress a hyperspectral data cube to meet the need of real-time process at a very low sampling rate，which consists of 3D circulant sampling and an efficient reconstruct algorithm with convergence guarantee. There are two major contributions in the paper. Firstly, circulant sampling is extended from 2D to 3D, utilizing the spectral correlation of HSI between the adjacent bands in the sampling process directly. Secondly, three-dimensional total variation (3DTV) is used as the regularization term to reconstruct HSI from the incomplete sampled data by taking advantage of the highly spatial and spectral correlation of HSI.

Experimental results demonstrate that our proposed 3DCS has a huge advantage on improving the image quality of reconstruct images. Even when the sampling rate decreases to a lower level, the method 3DCS can also give a better reconstruct image than 2DCS. The method presented here can be used widely in Hyperspectral CS techniques to reduce the measurement number and reduce the transmission and storage difficulties to meet the needs of real-time processing. Therefore, the method has a great significance on the design of the hyperspectral imaging spectrometer with a simpler hardware and a higher processing velocity.

Acknowledgment

The author thanks Prof. Feng for her constructive suggestions and would like to express her gratitude to all those who helped her during the writing of this thesis.

References

[1] D.Donoho, “Compressed sensing”, IEEE Trans. Inform. Theory, vol. 52, no. 2, pp. 489-509, 2006.

[2] R. Baraniuk, “A lecture on compressive sensing”, IEEE Signal Processing, vol.24, no.1, pp. 118-221, 2007.

[3] E Candès, J Romberg, Terence Tao, “Robust uncertainty principles: exact signal reconstruction from highly incomplete frequency information”, IEEE Transaction on Information Theory, vol. 52, no.2, 489-509, 2006.

[4] J. Romberg, “Compressive sensing by random convolution”, SIAM J. Imaging Sciences, 2009.

[5] W. Yin, S. P. Morgan, J. Yang, and Y. Zhang, “Practical compressive sensing with toeplitz and circulant matrices”, Rice University CAAM Technical Report TR10-01, 2010.

[6] M. Lustig, D. Donoho, J. Santos, and J. Pauly, “Compressed sensing mri”, IEEE Signal Processing Magazine, vol.25, no.2, pp.72–82, 2008.

[7] Q. Du and J. E. Fowler, “Hyperspectral image compression using jpeg2000 and principal component analysis”, IEEE Geosci. Remote Sens. Lett., vol.4, no.4, pp.201–205, 2007.

[8] J. E. Fowler and Q. Du, “Reconstructions from compressive random projections of hyperspectral imagery”, Optical Remote Sensing: Advances in Signal Processing and Exploitation Techniques, S. Prasad, L. M. Bruce, and J. Chanussot, Eds. Springer, pp.31-48, 2011.

[9] Mohammad Golbabaee, Simon Arberet and Pierre Vandergheynst, “Distributed compressed sensing of hyperspectral images via blind source separation”, 978-1-4244-9721-8/10, IEEE, pp.196-198, 2010.

[10] Haiying Liu, Chengke Wu, Lv Pei and Song Juan, “Compressed hyperspectral image sensing reconstruction based on interband prediction and joint optimization”, Journal of Electronics & Information Technology. vol.33, no.9, pp. 2248-2252, 2011.

[11] J Yang, Y Zhang, and W Yin, “A fast alternating direction method for TVL1-L2 signal reconstruction from partial fourier data”, IEEE journal of selected topics in signal processing, vol.4, no.2, pp.288-297, 2010.

[12] Yilun Wang, Junfeng Yang, Wotao Yin, and Yin Zhang, “A new alternating minimization algorithm for total variation image reconstruction”, SIAM J. Imaging Science, vol.1, no.3, pp. 248-272, 2008.

[13] X. Shu and N. Ahuja, “Hybrid compressive sampling via a new total variation tvl1”, Proc. of European Conference on Computer Vision, pp.393-404, 2010.

[14] M. Afonso, J. Bioucas-Dias, and M. Figueiredo, “Fast image recovery using variable splitting and constrained optimization”, IEEE Trans. Image Process., vol.19, no.9, pp. 2345–2356, 2010.